Journal of Artificial Intelligence and Data Mining (JAIDM), Vol. 11, No. 3, 2023, 477-485.

Shahrood University of Technology

Journal of Artificial Intelligence and Data Mining (JAIDM)

Journal homepage: http://jad.shahroodut.ac.ir

Research paper

Segmentation of Breast Cancer using Convolutional Neural Network and U-Net Architecture

Saiful Bukhori*, Muhammad Almas Bariiqy, Windi Eka Y. R and Januar Adi Putra

Computer Science Department, University of Jember, Indonesia.

Article Info

Article History:

Received 04 February 2023
Revised 26 March 2023
Accepted 05 June 2023

DOI:10.22044/jadm.2023.12676.2419

Keywords:

Breast Cancer, Convolutional Neural Network, U-Net, Mean IoU.

**Corresponding author: saiful.ilkom@unej.ac.id (S. Bukhori).*

Abstract

Breast cancer is a disease of abnormal cell proliferation in the breast tissue organs. One method for diagnosing and screening breast cancer is mammography. However, the results of this mammography image have limitations because it has a low contrast and a high noise, and contrast as non-coherence. This research work segmented breast cancer images derived from Ultrasonography (USG) photo using a Convolutional Neural Network (CNN) using the U-Net architecture. Testing on the CNN model with the U-Net architecture results in the highest Mean Intersection over Union (Mean IoU) value in the data scenario with a ratio of 70%:30% , 100 epochs, and a learning rate of $5 \ x \ 10^{-5}$, which is 77%, while the lowest Mean IoU in the data scenario with a ratio 90%:10% , 50 epochs, and a learning rate of $1 \ x \ 10^{-4}$ learning rate, which is 64.4%.

1. Introduction

Breast cancer is an abnormal cell proliferation in breast tissue organs that can occur due to ductal or lobular epithelium [1]. Breast cancer is one of the most common cancers in the world. The incidence of cancer is estimated at 2.26 million in 2020. Factors that contribute to the poor survival of cancer patients are delays in diagnosis and lack of effective access to treatment [2]. Improving the survival of cancer patients around the world can be increased by the existence of three pillars, namely: health promotion, timely diagnosis, and comprehensive treatment and supportive care [3]. Death and survival of the breast cancer patients is strongly influenced by timely diagnosis and the effectiveness of modalities treatment. One way to diagnose is by using mammography.

Mammography is used for diagnostics and screening. Mammography is an examination by emitting X-rays through the breast to a detector to be transmitted in the form of electronic signals that form digital images. The resulting image is called a mammogram [4]. Low-density tissue, such as fat, is translucent, while dense tissue such as breast cancer appears whiter against a gray background. Mammograms are used by doctors to analyze breast abnormalities [5]. Mammography can detect lumps in early-stage breast cancer that is still small [6]. However, the results of this mammography image have limitations because it has low contrast and high noise and contrast as non-coherence between regions. These factors make the diagnosis of breast cancer less valid [7]. This problem can be solved using image enhancement techniques so as to improve the overall process of breast cancer segmentation. After the image is enhanced, the stage of examining the shape, size and location of the cancer using the mammography method still requires visual interpretation so that this stage also causes inaccuracy, and is subjective due to differences in perceptions between health workers or radiologists. Thus, we need a technology that can help analyze ultrasound images quickly and accurately using computer vision and artificial intelligence.

This research work proposed segmentation of breast cancer images using computer vision and artificial intelligence to reduce the visual limitations of images and the subjectivity of health workers or radiologists. Several previous studies have used computer vision to detect breast cancer (although using different data) [8] [9] [10], some of them used machine learning [11] [12] [13] [14], while others used deep learning [15] [16] [17]. In this research work using the Multi-Layer Perceptron Neural Network (MLP) and Convolutional Neural Network (CNN) to diagnose breast cancer anatomy, especially the shape, size, and location of the cancer because the shape, size, and location of this cancer is needed for early detection of breast cancer. MLP is a neural network that consists of at least three layers, namely: input layer, hidden layer, and output layer [18]. CNN is a deep learning method that is used to identify digital images that consist of many layers that can be trained [19]. The output of each layer on the CNN is a feature map which consists of an array that represents the feature map for each level, input and output. The testing used Intersection over Union (IoU) to measure the overlap between two boundary objects or masks.

The CNN has a very fast development in the process of image classification, object detection, object localization, and image segmentation. Developments occurred in the modification of the CNN layer configuration into several types, namely the subsampling layer, convolutional layer, loss layer, and fully connected layer. This research work develops CNN to overcome problems in the biomedical field, especially breast cancer detection using image segmentation. Image segmentation is a method that divides the image into several parts based on the color similarity value of the pixels or divides the image between background and foreground [20].

U-Net is one of the CNN architectures in the field of image segmentation [21]. The U-Net architecture is designed for biomedical image segmentation by applying data augmentation, so that it can optimize the training process on small datasets. The U-Net architecture is divided into 3 parts, namely encoder, bottleneck, and decoder [22]. Previous studies have implemented the U-Net architecture for MRI-based brain tumor segmentation. This research combines the VGG-16 architecture with the U-Net architecture. The combination of VGG-16 architecture with U-Net with transfer learning for MRI-based brain tumor segmentation produces an accuracy rate of 96% better than the U-Net architecture alone with an accuracy of 93% [22]. The U-Net architecture on CNN developed in this study is an architecture for breast cancer segmentation, so that the shape, size, and location of the cancer can be identified by measuring the overlap between two boundary objects or masks using IoU.

The rest of this paper is organized as what follows. The proposed model and system design for segmentation of breast cancer using CNN and U-Net architecture is discussed in the methods section (Section 2). Section 3 discusses the results and analysis of CNN model. Finally, conclusions are given in Section 4.

2. Related Works

Image quality and feature extraction algorithms unreliable in detection of breast cancer due to noise. Ennam. G and Dr. Vemuri B.S. Srilatha Indira Dutt, D examined feature extraction using GLCM and then optimized it [23]. To prove its effectiveness compared to existing research [24] [25], this research work resulted in a high accuracy, which is 94% for the analogy between cancer and non-cancer cells. In this research used ultra-wideband (UWB) images obtained from different sources, with specimens of 100 images. 80% of the data was taken for training, and 20% of the data was used for testing. The intensity and texture features extracted were continued by inclusion in the Neural classifier proposed by Rahimeh *et al*. to classify benign and malignant mammograms [26]. The accuracy rate obtained is 96.47%. This research work used 93 ROI mammography containing 54 benign tumors and 39 malignant tumors from the MIAS database. This research work also uses 170 ROI mammography containing 74 benign tumors and 96 malignant tumors from the DDSM database. An algorithm for detecting suspicious masses from mammographic images by using a linear transformation enhancement filter for local contrast enhancement of each pixel and a local adaptive threshold technique used for image binarization subtracted from the original image containing the mass was proposed by G. Kom *et al*. [27]. The sensitivity of this proposed method reached up to 95.91% when it was tested on a set of 61 mammograms provided by the radiology department of the Yaounde Gynaeco–Obstetric and Pediatric Hospital (YGOPH). The breast mass detection system by means of image denoising using morphological top hat surgery, settling operation, Ostu thresholding and addition operation was proposed by Danilo *et al*. [28]. Images are decomposed into different resolutions using a 2DWT filter and an adaptive wiener filter is applied to the decomposed image to remove noise. The proposed method was quantitatively evaluated with images collected from the Digital Database for Screening Mammography (DDSM) in CC and MLO views where the mean ± standard deviation of the metric standard deviation area was $79.2 \pm 8\%$

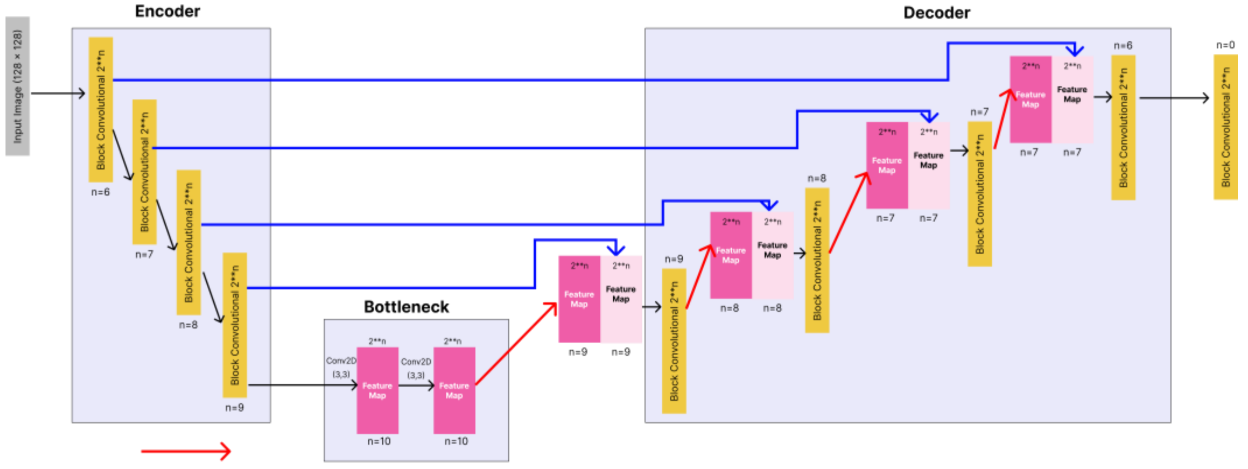

Figure 1. The Proposed System.

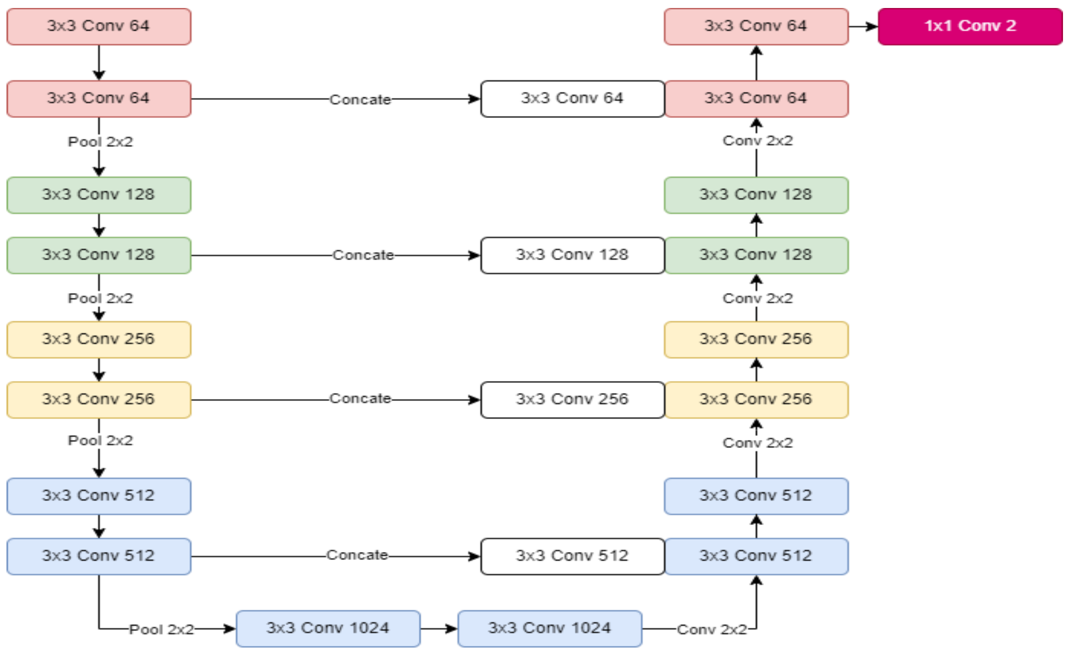

Figure 2. U-Net architecture.

3. Materials and Method

The architecture proposed in this research work is U-Net architecture on CNN for breast cancer segmentation, so that the shape, size, and location of the cancer can be identified by measuring the overlap between two boundary objects or masks using IoU. The architectural design is divided into 3 parts, namely encoder, bottleneck and decoder. The encoder is designed to consist of 4 convolution blocks with 2 convolutions with a size of 3*3 and a max pooling size of 2*2 with the number of filters for each encoder block 64, 128, 256, 512. Bottleneck is designed with 1 convolution block consisting of 2 convolutions with size 3*3, and the number of filters is 1024. The output is designed with a convolution size of 2*2 for up sampling. The decoder is designed with 4 convolution blocks consisting of 2 convolutions measuring 3*3 with the first layer of each block combined with the output of the encoder resulting block and using the convolution output with a size of 2*2, The filter for each decoder block is 512, 256, 128, 64. The output produced by the U-Net architecture is processed using a convolution with a size of 1*1 and the number of filters is 2. The proposed system in this research work is shown in Figure 1, and the U-Net Architecture is shown in Figure 2.

The U-Net architectural model that has been designed is tested to obtain the optimal model. Tests are carried out using the values of several parameters to achieve the best image segmentation results. The parameters tested are the number of epochs and the data test scenarios with the ratio between data training and data testing. The first scenario is used 2 different epochs, namely epoch 50 and epoch 100, while the second scenario is used 2 different ratios between data training and data testing, namely 70%:30% and 90%:10%. Experiments were also carried out by adding hyperparameter scenarios and 2 learning rate scenarios, namely 1×10^{-4} and 5×10^{-5}. The results of model testing are continued by comparing the Mean IoU matrix values of each model to select the model with the highest accuracy. The Mean IoU matrix calculation uses the Mean Intersect of Union equation, as follows:

$$Mean\ IoU = \frac{1}{C}\sum_{c} IoU_{c} \qquad (1)$$

If there is a system failure during model testing due to the unbalanced IoU matrix results, it will be repeated in the U-Net architectural design process. The data used as input in this research work is the Breast Ultrasound Images Dataset (BUSI Dataset) [29]. The BUSI dataset is categorized into three classes, namely normal, benign, and malignant. The dataset consists of 780 images of different women with an average image size of 500*500 pixels. Of the 780 tumor images, 133 normal images without cancer masses, 437 cancer mass images, and 210 benign mass images. In this research, 437 images of cancerous masses and 210 images of benign masses were used, so that the amount of data is 647 images. Sample image as shown in Figure 3.

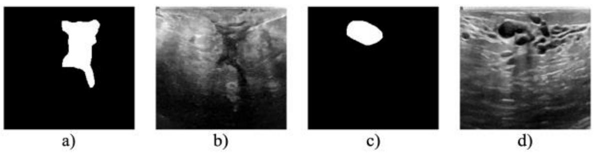

Figure 3. a) Malignant breast cancer ground truth images b) malignant breast cancer ultrasound images c) benign breast cancer ground truth images d) benign breast cancer ultrasound images.

Before the data is entered into the training process to avoid errors in classification, the dataset is adjusted manually, especially to adjust the brightness value per pixel. Incompatible data will be changed, and those that are appropriate will be used as the final, clean dataset. Compatible data is data that has the appropriate format, namely the extension (*.png), the appropriate position, if not, it will be rotated according to the correct position, the image is clear, and certain parts match the object under study; otherwise, it will be cut as needed. The U-Net architectural model designed in this research work is divided into three parts, namely the encoder, bottleneck, and decoder. The encoder is designed with 4 convolution blocks with 2^n filter sizes and each of n is, 6, 7, 8, 9. The value of n is the coefficient of the number of filters. The convolution block on the encoder section has 2 convolution layers with an activation function using *ReLU*, 1 Max Pooling layer (2*2) and 1 dropout layer of 20%, as shown in Figure 4. The last convolution block on the encoder has a convolution layer with a filter size of 512. The output of the last convolution layer on the encoder is a feature map with size 8*8, as shown in Figure 5.

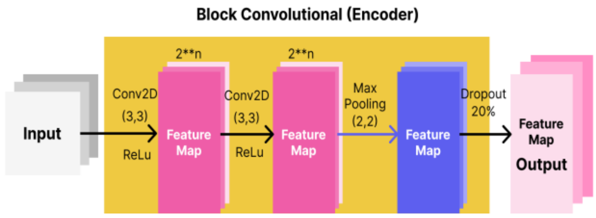

Figure 4. Convolution block (encoder).

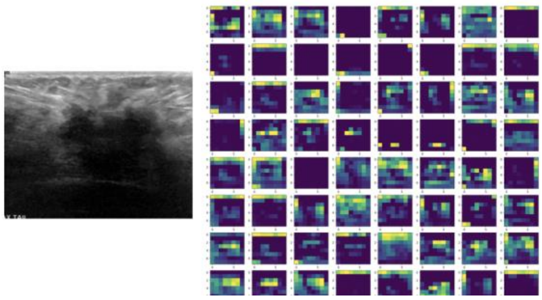

Figure 5. a) Input b) Feature map (encoder).

The bottleneck is designed with two convolution layers with a filter size of 2^n and $n = 10$. The value of n is the coefficient of the number of filters. The bottleneck feature map output is transposed to become a feature map with a feature value of 2^{n-1} Then it will be combined with the output feature map from the convolution block, which has the same number of filters, as shown in Figure 6. The last layer in the bottleneck has a convolution layer with a filter size of 1024. The output of the last convolution layer in the bottleneck is a feature map with size 8*8 , as shown in Figure 7.

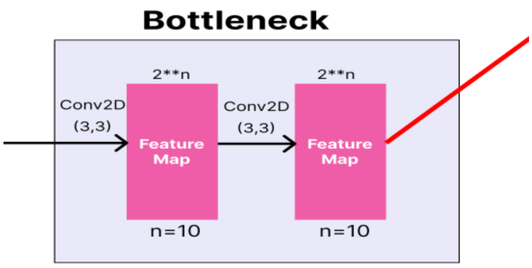

Figure 6. Bottleneck.

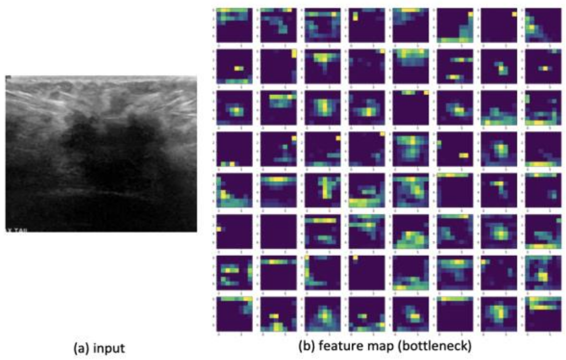

Figure 7. a) Input b) Feature map (bottleneck).

The decoder consists of two convolution layers with 2^n filter sizes and each of n is 9, 8, 7, 6. The value of n is the coefficient of the number of filters. The convolution layer on the decoder uses the *ReLU* activation function with a 10% dropout layer as shown in Figure 8. Before entering each convolution block in the encoder, the feature map processes sampling and combines the feature map input with the feature map output on the encoder convolution block, which has a total the same filters. The up-sampling process uses the transpose layer until the input filter size is equal to the convolution layer filter size. The last layer on the encoder is a convolution layer with a filter size of 64. The output of the last convolution layer on the encoder is a feature map with a size of 128*128 as shown in Figure 9.

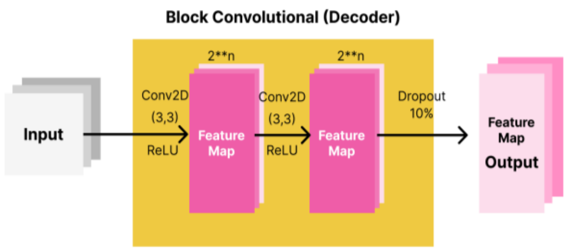

Figure 8. Convolution block (decoder).

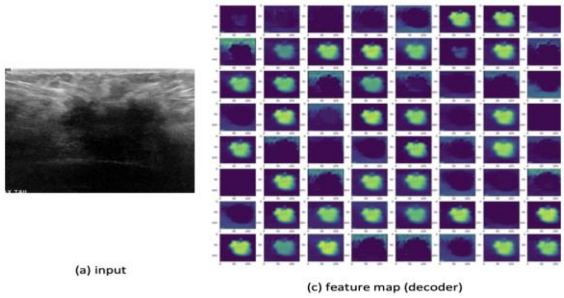

Figure 9. a) Input b) Feature map (decoder).

4. Results and Discussion

Testing on the CNN model using the U-Net architecture is calculated the accuracy of the model based on IoU. IoU is the intersection of the prediction results and the ground truth divided by the union of the predicted results and the ground truth. This process is carried out by comparing for different values of the epoch parameter, learning rate and scenario data training and data testing. This process is very important because the model will be selected for the scenario with the highest accuracy. Before comparing the accuracy, the model will be tested by scenario of data training and data testing. The scenario used 2 different ratios namely 70%:30% and 90%:10%. Scenario of data training and data testing was carried out to test the model with different epoch parameter values and different learning rates. The epoch parameter values used were 50 and 100.The comparison of learning rates were 1×10^{-4} and 5×10^{-5}. After the model is tested, the results of all scenarios are compared to get the best model scenario. Testing using a 70%:30% data scenario is carried out by adding 10 validation data inputs and breast cancer ultrasound image test data to predict the model. The prediction results of the USG image are compared with the ground truth using IoU calculations. A sample comparison of predicted images and ground truth images as shown in Figure 10. Image comparison values produce intersections and unions of ground truth images and predictive images, as shown in Table 1. Experiments using 10 malignant breast cancer data as samples obtained Mean IoU values, as shown in Table 2.

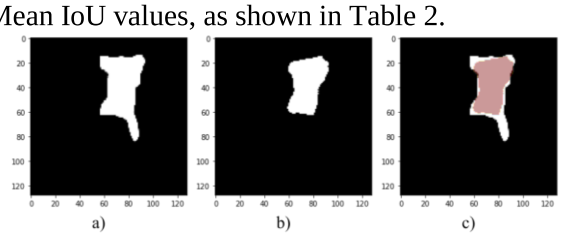

Figure 10. (a) Ground truth image (b) Predictive image (c) Combined ground truth image with predictive image.

Table 1. Intersection and union data 70%:30% .

Scenario	Intersection (pixels)	Union (pixels)	IoU
Epoch 50 learning rate 1×10^{-4}	1159	1594	0.727
Epoch 100 learning rate 1×10^{-4}	1151	1571	0.732
Epoch 50 learning rate 5×10^{-5}	977	1550	0.630
Epoch 100 learning rate 5×10^{-5}	1226	1584	0.773

Table 2. Mean IoU data 70%:30%   malignant cancer.

Scenario	Sample	IoU	Mean IoU
Epoch 50 *learning rate* 1×10^{-4}	sample 1	0.874	**0.739**
	sample 2	0.802	
	sample 3	0.547	
	sample 4	0.727	
	sample 5	0.795	
	sample 6	0.878	
	sample 7	0.749	
	sample 8	0.489	
	sample 9	0.737	
	sample 10	0.790	
Epoch 100 *learning rate* 1×10^{-4}	sample 1	0.787	**0.716**
	sample 2	0.753	
	sample 3	0.562	
	sample 4	0.732	
	sample 5	0.787	
	sample 6	0.904	
	sample 7	0.782	
	sample 8	0.459	
	sample 9	0.705	
	sample 10	0.691	
Epoch 50 *learning rate* 5×10^{-5}	sample 1	0.700	**0.709**
	sample 2	0.762	
	sample 3	0.479	
	sample 4	0.630	
	sample 5	0.806	
	sample 6	0.784	
	sample 7	0.629	
	sample 8	0.818	
	sample 9	0.734	
	sample 10	0.744	
Epoch 100 *learning rate* 5×10^{-5}	sample 1	0.819	**0.77**
	sample 2	0.793	
	sample 3	0.608	
	sample 4	0.773	
	sample 5	0.805	
	sample 6	0.899	
	sample 7	0.758	
	sample 8	0.770	
	sample 9	0.722	
	sample 10	0.752	

The test results show that the Mean IoU in the 100 epoch scenario and 5×10^{-5} in the malignant cancer data validation has a higher accuracy value in the 70%:30% data comparison. Meanwhile, the Mean IoU for the data test used is shown in Table 3.

Table 3. Mean IoU data test 70%:30%.

Scenario	Sample	Mean IoU
Epoch 50 learning rate 1×10^{-4}	191 Sample	0.58
Epoch 100 learning rate 1×10^{-4}	191 Sample	0.64
Epoch 50 learning rate 5×10^{-5}	191 Sample	0.47
Epoch 100 learning rate 5×10^{-5}	191 Sample	0.62

The testing process on the 70%:30% data scenario has a graph that tends to be normal for the epoch 50 scenario, while the epoch 100 scenario experiences a bit of overfitting in the process of epoch 50 to epoch 100 even though the difference between training loss and validation loss is almost the same. A sample of the output comparison of image predictions and ground truth images in the testing process the 70%:30% data scenario, as shown in Figure 11, and the graph of the training process in the 70%:30% data scenario is shown in Figure 12.

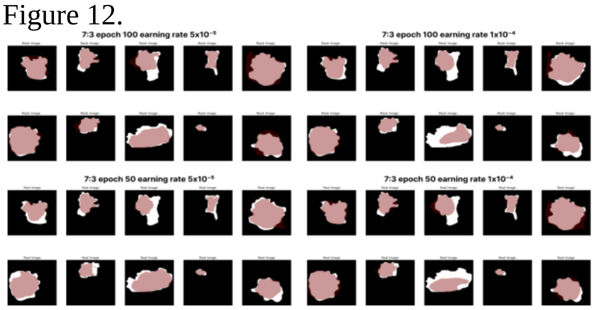

Figure 11. Ground truth image, predictive image, and combined ground truth image with predictive image in the testing process the 70%:30% data scenario.

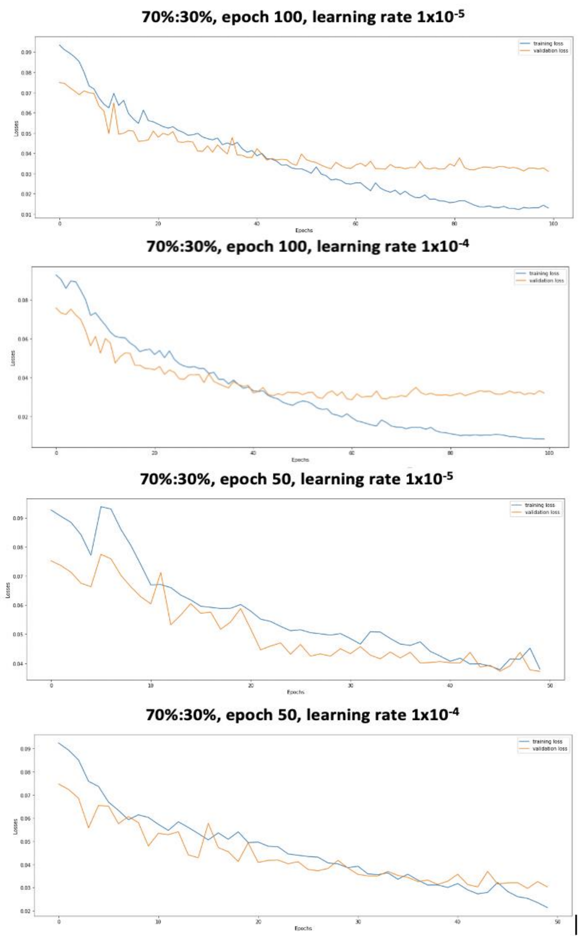

Figure 12. Graph of training on data scenario 70%:30% .

The second test using a 90%:10% data scenario was carried out by adding 10 data validation for breast cancer ultrasound images to be predicted by the model. Prediction results from ultrasound images will be compared with ground truth using IoU. Image comparison values produce intersections and unions of ground truth images and predictive images, as shown in the Table 4. Experiments using 10 malignant breast cancer data as samples obtained Mean IoU values, as shown in Table 5.

Table 4. Intersection and union data 90%:10% .

Scenario	Intersection (pixels)	Union (pixels)	IoU
Epoch 50 *learning rate* 1×10^{-4}	1018	1567	0.727
Epoch 100 *learning rate* 1×10^{-4}	1070	1650	0.732
Epoch 50 *learning rate* 5×10^{-5}	1199	1654	0.630
Epoch 100 *learning rate* 5×10^{-5}	1113	1571	0.773

Table 5. Mean IoU data 90% : 10% malignant cancer.

Scenario	Sample	IoU	Mean IoU
Epoch 50 *learning rate* 1×10^{-4}	sample 1	0.787	**0.644**
	sample 2	0.775	
	sample 3	0.511	
	sample 4	0.649	
	sample 5	0.468	
	sample 6	0.791	
	sample 7	0.710	
	sample 8	0.227	
	sample 9	0.735	
	sample 10	0.782	
Epoch 100 *learning rate* 1×10^{-4}	sample 1	0.854	**0.682**
	sample 2	0.745	
	sample 3	0.638	
	sample 4	0.648	
	sample 5	0.800	
	sample 6	0.904	
	sample 7	0.838	
	sample 8	0.042	
	sample 9	0.590	
	sample 10	0.757	
Epoch 50 *learning rate* 5×10^{-5}	sample 1	0.819	**0.748**
	sample 2	0.787	
	sample 3	0.569	
	sample 4	0.724	
	sample 5	0.878	
	sample 6	0.894	
	sample 7	0.720	
	sample 8	0.531	
	sample 9	0.756	
	sample 10	0.802	
Epoch 100 *learning rate* 5×10^{-5}	sample 1	0.848	**0.705**
	sample 2	0.785	
	sample 3	0.541	
	sample 4	0.708	
	sample 5	0.817	
	sample 6	0.901	
	sample 7	0.771	
	sample 8	0.158	
	sample 9	0.708	
	sample 10	0.808	

The test results show that the Mean IoU in the 50 epoch scenario and 5×10^{-5} in the malignant cancer data validation has a higher accuracy value in the 90%:10% data comparison. Meanwhile, the Mean IoU for the data test used is shown in Table 6.

Table 6. Mean IoU data test 90%:10% .

Scenario	Sample	Mean IoU
Epoch 50 *learning rate* 1×10^{-4}	64 Sample	0.66
Epoch 100 *learning rate* 1×10^{-4}	64 Sample	0.68
Epoch 50 *learning rate* 5×10^{-5}	64 Sample	0.62
Epoch 100 *learning rate* 5×10^{-5}	64 Sample	0.66

The testing process in the 90%:10% data scenario has a graph that is almost the same as the 70%:10% data comparison, which tends to be normal for the epoch 50 scenario, while the epoch 100 scenario experiences a bit of overfitting in epoch 50 to epoch 100, despite the difference in training loss and validation loss almost the same. A sample of the output comparison of image predictions and ground truth images in the testing process the 90%:10% data scenario as shown in Figure 13 and the graph of the training process in the 90%:10% data scenario is shown in Figure 14.

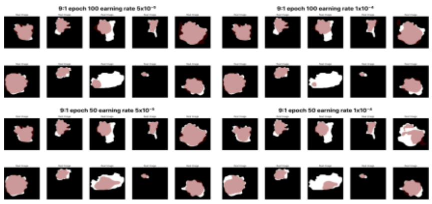

Figure 13. Ground truth image, predictive image, and combined ground truth image with predictive image in the testing process the 90%:10% data scenario.

The U-Net architectural model has been tested in each scenario with a comparison of training data and testing data, the number of epoch and different learning rates. Even though the model used is the same, the performance of the mean IoU value on the U-Net architectural model is different. Overall, the experimental results are as shown in Table 7.

Testing on the CNN model uses the U-Net architecture using various scenarios including ratio scenarios between training data and testing data, scenarios of the number of epochs, and the learning rate will get the model with the most optimal Mean IoU value. Image enhancement which consists of searching for the best contrast value and best noise removal is a relatively subjective processing technique, therefore experiments are needed for each object and for each specific purpose to obtain the most optimal model. Especially for the anatomical diagnosis of breast cancer, it is necessary to increase the amount of experimental data so that it can identify optimally, especially the shape, size and location of the cancer. This model needs to be developed for other objects and purposes by increasing the number of experiments using the same process.

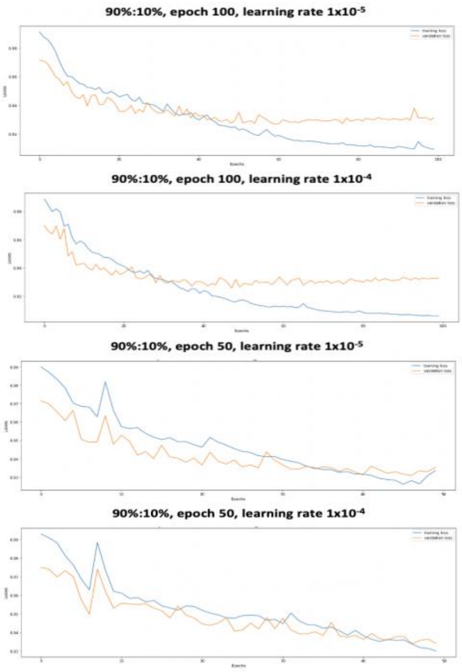

Figure 14. Graph of training on data scenario 90%:10% .

Table 7. Performance of Mean IoU.

Learning rate	Epoch	
	Epoch = 50	Epoch = 100
Ratio of training data and testing data (90% : 10%)		
Learning rate 1×10^{-4}	73.9%	71.6%
Learning rate 5×10^{-5}	70.9%	77%
Ratio of training data and testing data (90%:10%)		
Learning rate 1×10^{-4}	64.4%	68.2%
Learning rate 5×10^{-5}	74.8%	70.5%

5. Conclusion

Testing the accuracy of the U-Net architecture segmentation model is carried out by training the model using training data and testing the accuracy of the model using test data. The better the model is designed, the better the accuracy obtained. The test results show that the U-Net architecture model gets the results of the CNN model test, which has the highest Mean IoU value in the 70%:30% data scenario with 100 epochs and the learning rate value is 5×10^{-5}, which is 77%. Meanwhile, the lowest result is testing the data scenario of 90%:30% with 50 epochs and a learning rate of 1×10^{-4}, which is 64.4%. Based on the Mean IoU value, it indicates that using a 70%:30% scenario with 100 epochs and learning rate of 5×10^{-5} has the most optimal value. This architectural model is used in implementing the web app because it has the best accuracy among models with other scenarios.

References

[1] Y. Feng *et al.*, "Breast cancer development and progression: Risk factors, cancer stem cells, signaling pathways, genomics, and molecular pathogenesis," *Genes Dis.*, vol. 5, no. 2, pp. 77–106, 2018, doi: 10.1016/j.gendis.2018.05.001.

[2] K. Unger-Saldaña, "Challenges to the early diagnosis and treatment of breast cancer in developing countries," *World J. Clin. Oncol.*, vol. 5, no. 3, pp. 465–477, 2014, doi: 10.5306/wjco.v5.i3.465.

[3] S. Kumar and G. S. Preetha, "Health promotion: An effective tool for global health," *Indian J. Community Med.*, vol. 37, no. 1, pp. 5–12, 2012, doi: 10.4103/0970-0218.94009.

[4] L. Heck and J. Herzen, "Recent advances in X-ray imaging of breast tissue: From two- to three-dimensional imaging," *Phys. Medica*, vol. 79, no. September, pp. 69–79, 2020, doi: 10.1016/j.ejmp.2020.10.025.

[5] K. Loizidou, G. Skouroumouni, C. Nikolaou, and C. Pitris, "A Review of Computer-Aided Breast Cancer Diagnosis Using Sequential Mammograms," *Tomogr. (Ann Arbor, Mich.)*, vol. 8, no. 6, pp. 2874–2892, 2022, doi: 10.3390/tomography8060241.

[6] T. S. Menes, D. Coster, D. Coster, and S. Shenhar-Tsarfaty, "Contribution of clinical breast exam to cancer detection in women participating in a modern screening program," *BMC Womens. Health*, vol. 21, no. 1, pp. 1–8, 2021, doi: 10.1186/s12905-021-01507-x.

[7] L. Fakharzadeh, S. J. Hosseini, N. N. AKBARI, S. Khazni, and ..., "The Effect of Employing Clinical Teaching Associate Model on Cognitive Learning and Clinical Skills of Nursing Students," *Int. J. Sci. Study*, No. January 2018, 2017, doi: 10.17354/ijssNov/2017/51.

[8] H. Aljuaid, N. Alturki, N. Alsubaie, L. Cavallaro, and A. Liotta, "Computer-aided diagnosis for breast cancer classification using deep neural networks and transfer learning," *Comput. Methods Programs Biomed.*, vol. 223, p. 106951, 2022, doi: 10.1016/j.cmpb.2022.106951.

[9] D. A. Zebari *et al.*, "Systematic Review of Computing Approaches for Breast Cancer Detection Based Computer Aided Diagnosis Using Mammogram Images," *Appl. Artif. Intell.*, vol. 35, no. 15, pp. 2157–2203, 2021, doi: 10.1080/08839514.2021.2001177.

[10] A. A. Almazloum, A. R. Al-Hinnawi, R. De Fazio, and P. Visconti, "Assessment of Multi-Layer Perceptron Neural Network for Pulmonary Function Test's Diagnosis Using ATS and ERS Respiratory Standard Parameters," *Computers*, vol. 11, no. 9, 2022, doi: 10.3390/computers11090130.

[11] E. Mahoro and M. A. Akhloufi, "Applying Deep Learning for Breast Cancer Detection in Radiology," *Curr. Oncol.*, vol. 29, no. 11, pp. 8767–8793, 2022, doi: 10.3390/curroncol29110690.

[12] A. Patil and M. Rane, "Convolutional Neural Networks: An Overview and Its Applications in Pattern Recognition," *Smart Innov. Syst. Technol.*, vol. 195, pp. 21–30, 2021, doi: 10.1007/978-981-15-7078-0_3.

[13] O. Prentkovskis, J. Brezina, I. Konovalenko, P. Maruschak and J. Brezinová, "Research of U-Net-Based CNN Architectures for Metal Surface Defect Detection" *Machines*, vol. 251, no. 2, p. 24, 2022, doi: 10.1201/b15870-17.

[14] S. Bukhori, S. D. Maysaroha, and J. Adi, "Classification of Breast Cancer Tumors using a Random Forest on Mammogram Images," vol. 45, no. 1, pp. 6–17, 2023.

[15] R. Ramadan and S. Aly, "CU-Net: A New Improved Multi-Input Color U-Net Model for Skin Lesion Semantic Segmentation," *IEEE Access*, vol. 10, pp. 15539–15564, 2022, doi: 10.1109/ACCESS.2022.3148402.

[16] T. Falk *et al.*, "U-Net: deep learning for cell counting, detection, and morphometry," *Nat. Methods*, vol. 16, no. 1, pp. 67–70, 2019, doi: 10.1038/s41592-018-0261-2.

[17] A. Huang, L. Jiang, J. Zhang, and Q. Wang, "Attention-VGG16-UNet: a novel deep learning approach for automatic segmentation of the median nerve in ultrasound images," *Quant. Imaging Med. Surg.*, vol. 12, no. 6, pp. 3138–3150, 2022, doi: 10.21037/qims-21-1074.

[18] A. Hashemi Fath, F. Madanifar, and M. Abbasi, "Implementation of multilayer perceptron (MLP) and radial basis function (RBF) neural networks to predict solution gas-oil ratio of crude oil systems," *Petroleum*, vol. 6, no. 1. pp. 80–91, 2020. doi: 10.1016/j.petlm.2018.12.002.

[19] C. L. Fan and Y. J. Chung, "Design and Optimization of CNN Architecture to Identify the Types of Damage Imagery," *Mathematics*, vol. 10, no. 19, 2022, doi: 10.3390/math10193483.

[20] Y. Yu *et al.*, "Techniques and Challenges of Image Segmentation: A Review," *Electron.*, vol. 12, no. 5, 2023, doi: 10.3390/electronics12051199.

[21] M. Z. Alom, M. Hasan, C. Yakopcic, T. M. Taha, and V. K. Asari, "Recurrent Residual Convolutional Neural Network based on U-Net (R2U-Net) for Medical Image Segmentation," *J. Med. Imaging*, vol. 6, no. 1, pp. 014006-1-014006–16, 2019, doi: 10.1117/1.JMI.6.1.014006.

[22] X. X. Yin, L. Sun, Y. Fu, R. Lu, and Y. Zhang, "U-Net-Based Medical Image Segmentation," *J. Healthc. Eng.*, vol. 2022, 2022, doi: 10.1155/2022/4189781.

[23] E. Govinda and V. BSSrilatha Indira Dutt, "Breast Cancer Detection Using UWB Imaging and Convolutional Neural Network," *Ilkogr. Online-Elementary Educ. Online, Year*, vol. 20, no. 5, pp. 1657–1670, 2021, doi: 10.17051/ilkonline.2021.05.181.

[24] X. Zhang *et al.*, "Classification of whole mammogram and tomosynthesis images using deep convolutional neural networks," *IEEE Trans. Nanobioscience*, vol. 17, no. 3, pp. 237–242, 2018, doi: 10.1109/TNB.2018.2845103.

[25] M. H. Yap *et al.*, "Automated Breast Ultrasound Lesions Detection Using Convolutional Neural Networks," *IEEE J. Biomed. Heal. Informatics*, vol. 22, no. 4, pp. 1218–1226, 2018, doi: 10.1109/JBHI.2017.2731873.

[26] R. Rouhi, M. Jafari, S. Kasaei, and P. Keshavarzian, "Benign and malignant breast tumors classification based on region growing and CNN segmentation," *Expert Syst. Appl.*, vol. 42, no. 3, pp. 990–1002, 2015, doi: 10.1016/j.eswa.2014.09.020.

[27] G. Kom, A. Tiedeu, and M. Kom, "Automated detection of masses in mammograms by local adaptive thresholding," *Comput. Biol. Med.*, vol. 37, no. 1, pp. 37–48, 2007, doi: 10.1016/j.compbiomed.2005.12.004.

[28] D. C. Pereira, R. P. Ramos, and M. Z. do Nascimento, "Segmentation and detection of breast cancer in mammograms combining wavelet analysis and genetic algorithm," *Comput. Methods Programs Biomed.*, vol. 114, no. 1, pp. 88–101, 2014, doi: 10.1016/j.cmpb.2014.01.014.

[29] W. Al-Dhabyani, G. Gomaa, H. Khaled and A. Fahmy, "Dataset of breast ultrasound images," *Data Brief.*, 2020, doi: 10.1016/j.dib.2019.104863.

تقسیم‌بندی سرطان پستان با استفاده از شبکه عصبی کانولوشن و معماری U-Net

Saiful Bukhori* ، Almas Bariiqy Muhammad ، Windi Eka Y. R و Januar Adi Putra

گروه علوم کامپیوتر، دانشگاه جمبر، اندونزی.

ارسال ۲۰۲۳/۰۲/۰۴؛ بازنگری ۲۰۲۳/۰۳/۲۶؛ پذیرش ۲۰۲۳/۰۶/۰۵

چکیده:

سرطان سینه یک بیماری تکثیر غیر طبیعی سلولی در اندام‌های بافت پستان است .یکی از روش‌های تشخیص و غربالگری سرطان سینه ماموگرافی است. اما نتایج این تصویر ماموگرافی دارای محدودیت‌هایی است زیرا کنتراست کم و نویز بالا دارند و کنتراست به عنوان عدم پیوستگی است .این کار تحقیقاتی تصاویر سرطان سینه حاصل از عکس اولتراسونوگرافی (USG) را با استفاده از یک شبکه عصبی کانولوشنال (CNN) با استفاده از معماری U-Netتقسیم‌بندی کرده است .آزمایش بر روی مدل CNN با معماری U-Net منجر به بالاترین مقدار میانگین تقاطع بیش از اتحادیه (Mean IoU) در سناریوی داده با نسبت ۷۰٪:۳۰٪، ۱۰۰ دوره و نرخ یادگیری $5 \; x \; 10^{-5}$ ۷۷ ٪می‌شود ، در حالی که کمترین میانگین IoU در سناریوی داده با نسبت ۹۰٪:۱۰٪، ۵۰ دوره و نرخ یادگیری $1 \; x \; 10^{-4}$ است که نرخ یادگیری ۶۴,۴٪ است.

کلمات کلیدی: سرطان پستان، شبکه عصبی کانولوشن، U-Net، میانگین IoU.